



HAL
open science

Dependence of basic creep on the relative humidity

Jean Michel Torrenti, Nedjar Boumediene, Aili Abudushalamu

► **To cite this version:**

Jean Michel Torrenti, Nedjar Boumediene, Aili Abudushalamu. Dependence of basic creep on the relative humidity. fib 2023 Symposium Istanbul, Jun 2023, Istanbul, Turkey. pp.246-253, 10.1007/978-3-031-32519-9_23 . hal-04099577

HAL Id: hal-04099577

<https://hal.science/hal-04099577v1>

Submitted on 17 May 2023

HAL is a multi-disciplinary open access archive for the deposit and dissemination of scientific research documents, whether they are published or not. The documents may come from teaching and research institutions in France or abroad, or from public or private research centers.

L'archive ouverte pluridisciplinaire **HAL**, est destinée au dépôt et à la diffusion de documents scientifiques de niveau recherche, publiés ou non, émanant des établissements d'enseignement et de recherche français ou étrangers, des laboratoires publics ou privés.

Dependence of basic creep on the relative humidity

Torrenti Jean Michel¹[0000-0003-0467-4371], Nedjar Boumediene²[0000-0002-2227-258X] and Aili Abudushalamu³[0000-0003-0780-8734]

¹ Univ Gustave Eiffel, France
jean-michel.torrenti@univ-eiffel.fr

² Univ Gustave Eiffel, France

³ Nagoya University, Japan

Abstract. The prediction of delayed strains is particularly important for prestressed structures. In modern codes like the fib MC2010, the delayed strains are split into four components: autogenous shrinkage, drying shrinkage, basic creep, and drying creep. Basic creep is the creep of a concrete sample in a test where drying is avoided. When drying is allowed, drying creep is the difference between the total strain minus the total shrinkage and the basic creep.

However, in the drying creep test, the relative humidity (RH) is lower than the RH of the test performed to measure the basic creep. And there are several experimental pieces of evidence showing that, when the RH is lower, basic creep is reduced: micro-indentation tests and creep tests on large samples with an initial drying to lower the internal RH. In the first part of the paper, we analyze these tests and propose a relation for RH-dependent basic creep. In the second part of the paper, the consequences of this dependence on the evaluation of drying creep are discussed by using FEM simulations for the modelling of the total creep test and considering the drying phenomenon.

Keywords: Concrete, creep, basic creep, relative humidity.

1 Introduction – Influence of RH on basic creep

The prediction of delayed strains is particularly important for prestressed structures like bridges or nuclear power plants. In modern codes like the fib MC2010 [1], the delayed strains are split into four components: autogenous shrinkage, drying shrinkage, basic creep, and drying creep. Basic creep is the creep of a concrete sample in a test where drying is avoided. It is the difference between the strain of a sealed loaded specimen and the autogenous shrinkage. When drying is allowed, drying creep is the difference between the total strain minus the total shrinkage and the basic creep.

But, in the drying creep test, the relative humidity (RH) is lower than the RH of the test performed to measure the basic creep. And there are several experimental pieces of evidence showing that, when the RH is lower, basic creep is reduced. Abiar [2] has compared the basic creep of a sample that was pre-dried with the classic basic creep.

Figure 1 shows that when the sample was pre-dried the basic creep was very small. Wittmann [3] has also performed basic creep tests on cement paste samples that were pre-dried at 105°C then stored in climatic chambers at different relative humidities for at least 3 months and tested only the specimens that did not change their weight. The creep tests were also performed with the corresponding imposed RH for each specimen. It is also clear here that the initial relative humidity has a strong influence on the basic creep, i.e. see Figure 2.

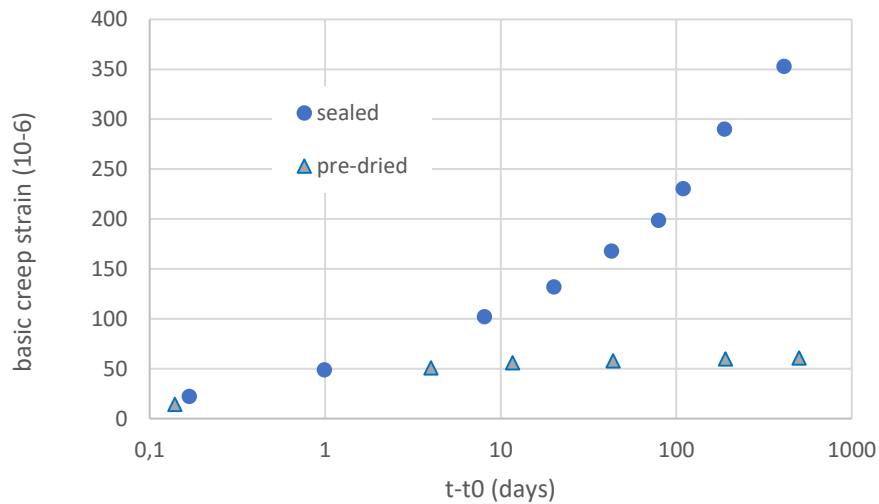


Fig. 1. Basic creep tests of sealed and pre-dried concretes (from Abiar [2])

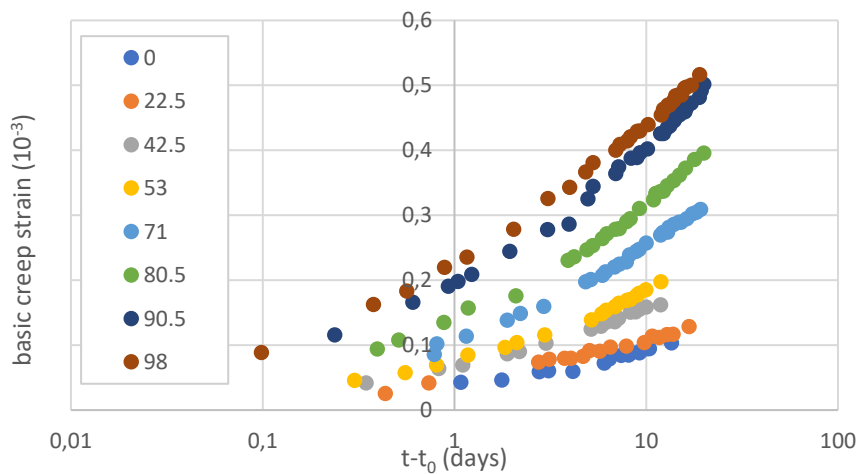


Fig. 2. Basic creep tests of cement paste specimen at different RH (from Wittmann [3])

Indeed, the water content plays an important role in the delayed deformations of concrete. Concerning basic creep, several theories are existing to explain this phenomenon: Bazant et al. [4] explained it with the famous micro-prestress theory in which the origin of the creep is the shear slip at overstressed creep sites and, recently, Vandamme [5] has proposed basic creep originates from local microscopic relaxations. And the presence of water is an important factor in these phenomena.

The macroscopic basic creep compliance follows a logarithmic evolution of the form:

$$J_{bc} = \frac{1}{C} \ln \left(1 + \frac{t-t_0}{\tau(t_0)} \right) \quad (1)$$

where J_{bc} is the basic creep compliance, C is a parameter that is homogenous to a basic creep modulus, t_0 is the age at loading, $t - t_0$ is the duration of loading, and $\tau(t_0)$ is a characteristic time depending on the age of loading. There is several experimental evidence of this logarithmic evolution in laboratory tests, see for instance [6,7], in real structures like bridges [8], or nuclear containments [9].

2 Results of micro-indentation tests

Vandamme [5] has also shown that micro-indentation allows the determination of the basic creep modulus C in a short time because the characteristic time $\tau(t_0)$ is reduced thanks to the high stress generated during such a test. Several authors have studied the creep of concrete using a micro-indentation test with different relative humidities [10, 11, 12, 13]. Of course, the magnitude of the creep modulus depends on the tested materials. But, it could be assumed that the variation of this parameter with RH is the same for all materials (i.e. the possible coupling between the material composition and the effect of RH is neglected). Figure 3 presents the evolution of the ratio $C(RH)/C(100\%)$ with RH. Despite a certain variability, there is a bi-linear trend in the evolution: between 80% and 100% RH the variation is limited while it is larger for RH below 80%. Equation (2) gives a possible relation for this evolution:

$$\frac{C(RH)}{C(100\%)} = \begin{cases} 1 + 0.1 \frac{(100-RH)}{20}, & 80\% < RH < 100\% \\ 1.1 + 2.1 \frac{(80-RH)}{80}, & 0 < RH < 80\% \end{cases} \quad (2)$$

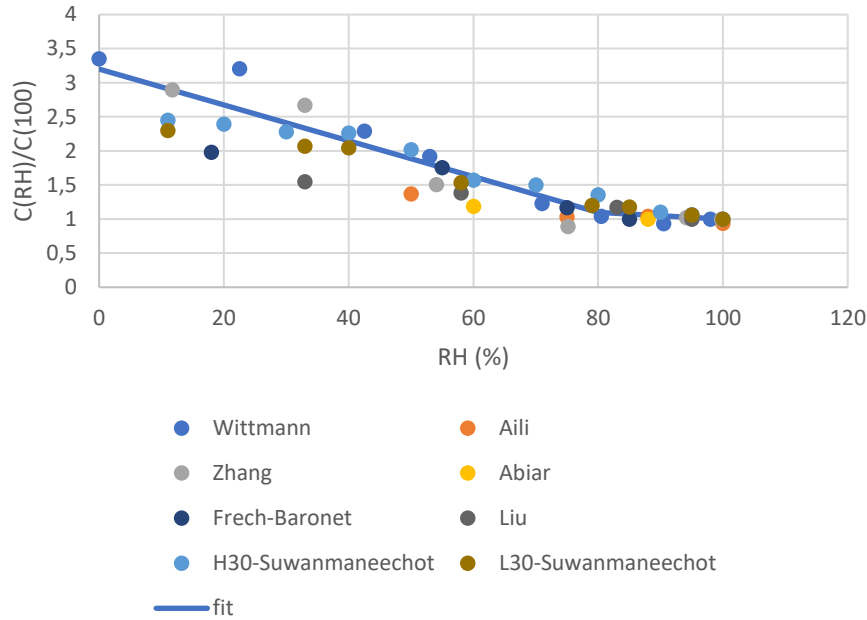


Fig. 3. Relation between the basic creep modulus and the relative humidity (creep tests from [2, 3 and 14], micro-indentation tests from [10, 11, 12, 13]).

3 Consequences for the creep of concrete

The fact that the basic creep modulus increases when RH decreases implies that during a creep test where drying is allowed, there is less basic creep than in a test where drying is prevented. The first consequence is that, since basic creep is dependent on drying, there is also a dependence of basic creep on the size of the concrete element (scale effect). The second consequence is that when drying creep is deduced by the subtraction of the basic creep from the total creep, there is an underestimation of the drying creep. It is not possible to know experimentally the error that is induced. In the following part of the paper, we will estimate such an error by a numerical simulation of the creep test of a drying specimen.

After modelling the drying of a concrete sample, the basic creep of a sealed sample is adjusted on experimental results. The results of the concrete of the VeRCoRs experiment are used here [9, 15]. Then the basic creep of the same concrete when drying occurs is estimated.

4 Modelling

As an application of the above findings, we choose to simulate a VerRCorRs test: the drying of a cylindrical sample of diameter $D = 16\text{cm}$ and height $H = 1\text{m}$, mechanically submitted to a constant compression of magnitude 12MPa during almost two years. To this end, a coupled hydro-mechanical resolution procedure is performed; a hydric problem for the drying evolution part, followed by a mechanical part that takes into account the RH-dependent creep phenomenon.

4.1 Modelling of the drying part of the test

The primary unknown of the problem is chosen to be the RH-field that we denote here for convenience by $h(\mathbf{x},t)$, and that is governed by the following transient equation,

$$\frac{\partial S(h)}{\partial t} + \text{div}[-d(h) \nabla h] = 0 \quad (3)$$

where $S(h)$ is the saturation function deduced from the desorption isotherm curve. This latter is herein approximated by the Hailwood-Horrobin function as,

$$S(h) = \frac{h}{F_1 + F_2 h + F_3 h^2} \quad (4)$$

with $F_3 = 1 - F_1 - F_2$, and where F_1 and F_2 are adimensional constants.

Moreover, in Eq. (3), $d(h)$ is the hydric diffusion coefficient that depends on the relative humidity. It is chosen as,

$$d(h) = B e^{Ah} \quad (5)$$

where A and B are parameters to be fitted with the concrete weight loss data obtained experimentally. To evaluate this water mass loss, we need to know the value of the water content at $h = 100\%$, and that we denote by W_{100} .

For the finite element simulations, the axisymmetry of the problem is exploited. The sample domain we consider is of height $H = 1\text{m}$ and radius $R = 8\text{cm}$. The finite element discretization we use consists of 300 quadrilateral linear elements: 30 elements radially, and 10 elements along the axis of the sample.

The initial condition is set to $h(\mathbf{x}, t = 0) = 100\%$. For the boundary conditions, a relative humidity $h_{\text{ext}} = 50\%$ is prescribed on the lateral surface during the whole simulation, and the sample is isolated at the top and bottom faces. Hence, the diffusion problem is purely radial. Table 1 summarized the material parameters used for the drying part of the numerical simulation.

Table 1. Material parameters used for the hydric part of the problem.

Parameters		
Saturation function $S(h)$, Eq. (4)	$F_1 = 1.335$	$F_2 = 1.391$
Hydric diffusion $d(h)$, Eq. (5)	$B = 11.75 \cdot 10^{-9} \text{mm}^2/\text{day}$	$A = 24.25$
Water content at $h = 100\%$	$W_{100} = 163 \text{l/m}^3$	

The predicted curve of water mass loss is plotted in Figure 4. A good agreement is to be noticed when comparing with the experimental data at our disposal. For the sake of illustration, Figure 5 shows the computed RH-field at two different times.

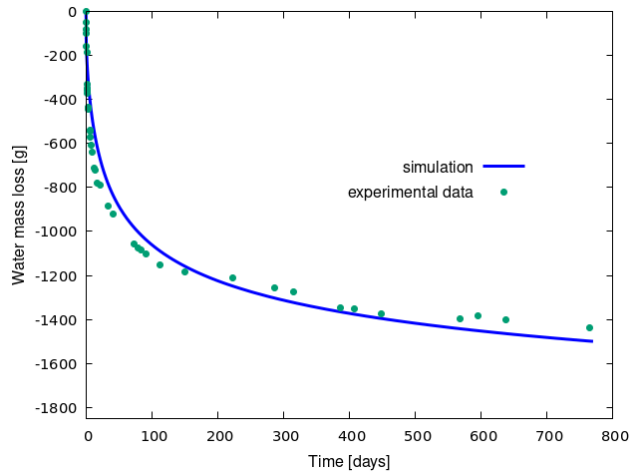


Fig. 4. Water mass loss of the cylindrical concrete sample. Experimental data and simulated curve issued from the FEM computation.

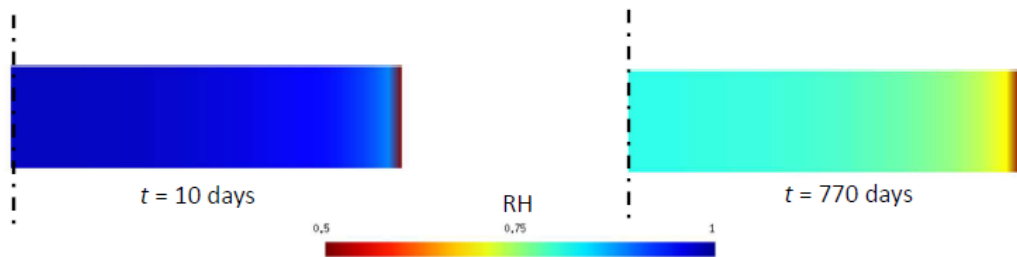


Fig. 5. Simulated relative humidity fields at two different times: at $t = 10$ days (left), and at $t = 770$ days (right).

4.2 Modelling of the basic creep when drying occurs

For the mechanical part of the problem, the basic creep strain tensor ε_{bc} is here treated as an internal variable, see for instance [16, 17] for analogies. The way in which this internal variable evolves is motivated by the basic creep compliance given in Eq. (1). In this case the evolution equation that governs the basic creep strain in its one-dimensional version is given by:

$$\dot{\varepsilon}_{bc} + \frac{E}{C(t+\tau)} \varepsilon_{bc} = \frac{E}{C(t+\tau)} \varepsilon \quad (6)$$

where ε is the total strain, and E is the elastic Young modulus. Here C is the basic creep modulus discussed above, and τ is the initial characteristic time. These two parameters must be identified from the experimental data.

Now for the mechanical part of the problem, the above cylindrical sample is submitted to a constant compression of 12 MPa. For the boundary conditions, the bottom face is simply fixed in the vertical direction, and the lateral surface is free. For the elastic parameters, we use $E = 36$ GPa and a Poisson's ratio $\nu = 0.2$. We have identified the following creep parameters for an RH-independent analysis:

$$C \equiv C(100\%) = 149.6 \text{ GPa} \quad \text{and} \quad \tau = 11 \text{ days} \quad (7)$$

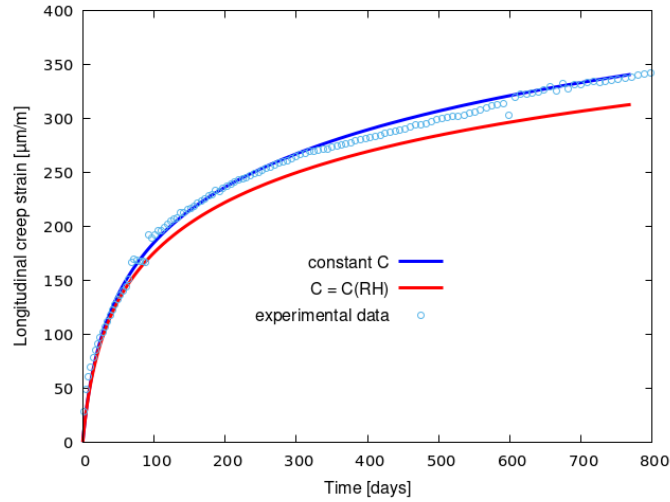


Fig. 6. Evolution of the longitudinal creep strain: (a) with the RH-independent creep model (blue curve), and (b) with the RH-dependent model as given by Eq. (2) (red curve).

With the parameters given in Eq. (7), the predicted creep evolution is plotted in Figure 6, blue curve. It is in good agreement with the experimental curve (dotted curve). On the other hand, when using the RH-dependent creep law as proposed in Eq. (2), the creep evolution is slightly different, see the red curve in Figure 7. This difference appears to grow with drying.

5 Conclusions

In modern calculation codes such as the fib model code 2020, the creep is the sum of two components: the basic creep and the desiccation creep. The latter is estimated by making the difference between the total creep measured on a drying specimen and the creep measured on a non-drying specimen. Such estimation implies that the basic creep is the same in these two specimens, even though their water contents are different. However, tests on specimens, confirmed by micro-indentation tests, have shown that basic creep depends on the water content of the cementitious material tested. The modelling framework described in this contribution allows considering the difference in creep amplitude with the RH-dependent evolution law. It shows that, in a test where the specimen dries, the basic creep is overestimated, which means that the drying creep is underestimated. As only the latter depends on the size of the parts, this can lead to an error in the prediction of delayed deformations in the very long term.

References

1. *fib*, (2012). "Fib Bulletin 65: Model Code 2010, Volume 1.
2. Abiar G., (1986). Cinétique de dessiccation et déformations différées du béton (analyse et modélisation), PhD thesis, Ecole nationale des ponts et chaussées (in French).
3. Wittmann, F. (1970). Einfluss des feuchtigkeitsgehaltes auf das kriechen des zementsteines. *rheologica Acta*, 9(2), 282-287.
4. Z.P. Bažant, A.B. Hauggaard, S. Baweja, F.-J. Ulm, Microprestress-solidification theory for concrete creep. I: Aging and drying effects, *J. Eng. Mech.* 123 (11) (1997) 1188–1194.
5. M. Vandamme, Two models based on local microscopic relaxations to explain long term basic creep of concrete, *Proc. R. Soc. A* 474 (2220) (2018) 20180477.
6. Le Roy, R., Le Maou, F., & Torrenti, J. M. (2017). Long term basic creep behavior of high performance concrete: data and modelling. *Materials and structures*, 50(1), 1-11.
7. Torrenti, J. M., & Le Roy, R. (2018). Analysis of some basic creep tests on concrete and their implications for modeling. *Structural Concrete*, 19(2), 483-488.
8. Bažant, Z. P., Hubler, M. H., & Yu, Q. (2011). Excessive creep deflections: An awakening. *Concrete international*, 8(33), 44-46.
9. Aili, A., & Torrenti, J. M. (2020). Modeling Long-term Delayed Strains of Prestressed Concrete with Real Temperature and Relative Humidity History. *Journal of Advanced Concrete Technology*, 18(7), 396-408.
10. Zhang, Q., Le Roy, R., Vandamme, M., & Zuber, B. (2014). Long-term creep properties of cementitious materials: Comparing microindentation testing with macroscopic uniaxial compressive testing. *Cement and Concrete Research*, 58, 89-98.

11. Frech-Baronet, J., Sorelli, L., & Charron, J. P. (2017). New evidences on the effect of the internal relative humidity on the creep and relaxation behaviour of a cement paste by micro-indentation techniques. *Cement and Concrete Research*, 91, 39-51.
12. Liu, Y., Li, Y., Jin, C., & Li, H. (2022). Multi-scale creep analysis of cement paste–Indentation prediction and time correspondence of mechanisms. *Cement and Concrete Composites*, 134, 104815.
13. Suwanmaneechot, P., Aili, A., & Maruyama, I. (2020). Creep behavior of CSH under different drying relative humidities: Interpretation of microindentation tests and sorption measurements by multi-scale analysis. *Cement and Concrete Research*, 132, 106036.
14. Aili A. (2017). Shrinkage and creep of cement-based materials under multiaxial load: poromechanical modeling for application in nuclear industry, PhD thesis, University Paris-Est
15. Charpin, L., Niepceron, J., Corbin, M., Masson, B., Mathieu, J. P., Haelewyn, J., ... & Torrenti, J. M. (2021). Ageing and air leakage assessment of a nuclear reactor containment mock-up: VERCORS 2nd benchmark. *Nuclear Engineering and Design*, 377, 111136.
16. Nedjar, B., & Le Roy, R. (2013). An approach to the modeling of viscoelastic damage. Application to the long-term creep of gypsum rock materials. *International Journal for Numerical and Analytical Methods in Geomechanics*, 37(9), 1066-1078.
17. Nedjar, B. (2022). Incremental viscoelasticity at finite strains for the modelling of 3D concrete printing. *Computational Mechanics*, 69, 233-243.